# Potential improvements

# on benzo(a)pyrene (BaP) mapping

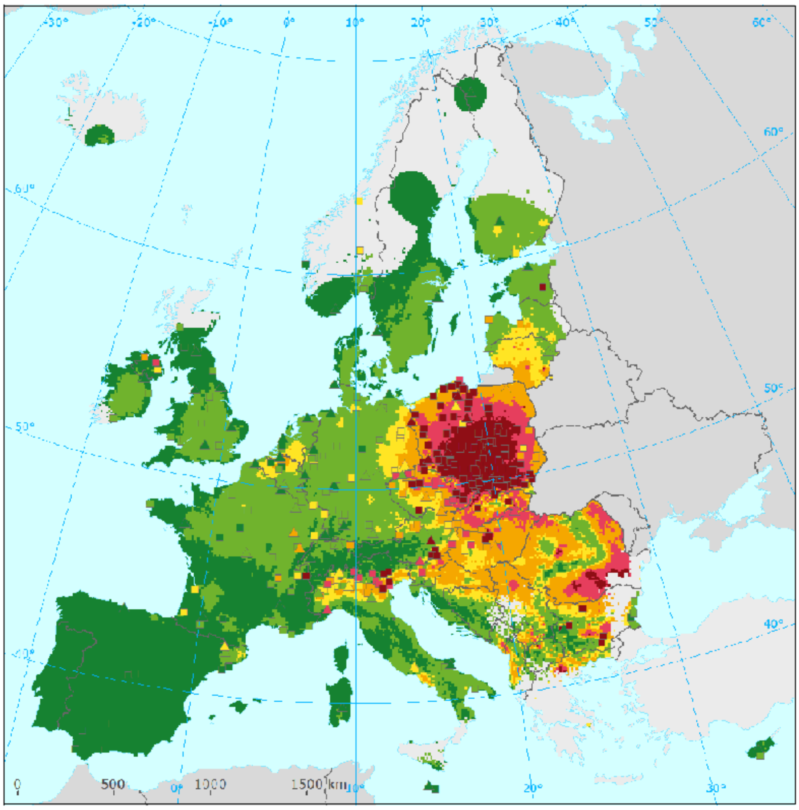

## ETC/ACM Technical Paper 2016/3

**September 2016**

*Jan Horálek, Cristina Guerreiro, Frank de Leeuw, Peter de Smet*

The European Topic Centre on Air Pollution and Climate Change Mitigation (ETC/ACM)
is a consortium of European institutes under contract of the European Environment Agency
RIVM Aether CHMI CSIC EMISIA INERIS NILU ÖKO-Institut ÖKO-Recherche PBL UAB UBA-V VITO 4Sfera

***Front page picture:***
*Main picture: Spatial interpolated concentration field of annual mean BaP in 2013, created by method (ii) using pseudo stations based on $PM_{10}$, limited for areas with a relative uncertainty under 0.60. Units: $ng.m^{-3}$. (This paper, Map 4.7, top.) This map variant gives the largest area with the acceptable uncertainty.*

***Author affiliation:***
*Jan Horálek: Czech Hydrometeorological Institute (CHMI), Prague, Czech Republic*
*Cristina Guerreiro: Norwegian Institute of Air Research (NILU), Kjeller, Norway*
*Frank de Leeuw, Peter de Smet: National Institute for Public Health and the Environment (RIVM), Bilthoven, The Netherlands*

## DISCLAIMER

This ETC/ACM Technical Paper has not been subjected to European Environment Agency (EEA) member country review. It does not represent the formal views of the EEA.


*ETC/ACM Technical Paper 2016/3*
*European Topic Centre on Air Pollution and Climate Change Mitigation*
*PO Box 1*
*3720 BA Bilthoven*
*The Netherlands*
*Phone +31 30 2748562*
*Fax +31 30 2744433*
*Email etcacm@rivm.nl*
*Website http://acm.eionet.europa.eu/*

# Contents

# 1 Introduction

Concentration levels of benzo(a)pyrene (BaP) are high across Europe and especially in central and eastern Europe, which may lead to a considerable risk to human health, although smaller compared to the health risk caused by $PM_{2.5}$. By combining observed, modelled and other supplementary data, a first European map of BaP was produced; see Guerreiro et al. (2015, 2016). This paper discusses potential improvements of that first map.

The mapping method is based primarily on air quality measurements. It combines monitoring data, chemical transport model results and other supplementary data, such as altitude and meteorology. The method consists of a linear regression model, followed by kriging of the residuals yielded from that model, i.e. the so called 'residual kriging'. Rural and urban background air quality is mapped separately; the final map is created by merging these two maps using a population density grid weighting.

However, the uncertainty of this final BaP map is very high, due to the limited number of BaP measuring stations. Trying to overcome this limitation, this report examines potential improvements of the BaP mapping and its exposure estimates by exploring the use of a "pseudo stations" data approach. The pseudo stations data approach is successfully applied in the regular $PM_{2.5}$ mapping (Denby et al., 2011; Horálek et al., 2016). Here we examine two options of the application of such pseudo-station approach for BaP mapping: one based on the data from $PM_{10}$ stations and another based on $PM_{2.5}$ stations.

Next to this, we examine as third alternative an approach which uses, as additional supplementary variables in the current method, the interpolated $PM_{2.5}$ rural and urban background maps as created routinely in the $PM_{2.5}$ mapping (Horálek et al., 2016).

Chapter 2 describes briefly the methodology applied. Chapter 3 documents the input data. Chapter 4 presents the analysis: Section 4.1 examines the pseudo BaP data method, while Section 4.2 compares the four different BaP mapping methods, i.e. (i) the current BaP mapping method, the methods with the pseudo BaP data from either (ii) $PM_{10}$ stations or (iii) $PM_{2.5}$ stations, and (iv) the alternative method utilizing the $PM_{2.5}$ rural and urban background maps as additional supplementary data. All calculations are based on 2013 data.

# 2 Methodology

## 2.1 Current mapping method

The current mapping methodology used to create the BaP concentration maps has been described in Guerreiro et al. (2015). In principle, this methodology is similar to the one we use for the regular mapping of PM and ozone, see e.g. Horálek et al. (2016). The air quality measurements are taken as the primary data source and the results from chemistry transport modelling and other auxiliary data (altitude, meteorology) as the secondary sources. The mapping method consists of a linear regression model followed by kriging of the residuals from that regression model (residual kriging):

$$\hat{Z}(s_0) = c + a_1 X_1(s_0) + a_2 X_2(s_0) + \ldots + a_n X_n(s_0) + \hat{\eta}(s_0), \tag{2.1}$$

where $\hat{Z}(s_0)$ is the estimated value of the air pollution indicator at a point $s_o$,

$X_1(s_0), X_2(s_0), \ldots, X_n(s_0)$ are $n$ individual supplementary variables at point $s_o$,

$c, a_1, a_2, \ldots, a_n$ are the $n+1$ parameters of the linear regression model calculated based on the data at the points of measurement,

$\hat{\eta}(s_0)$ is the spatial interpolation of the residuals of the linear regression model at point $s_o$, based on the residuals at the points of measurement.

The spatial interpolation of the regression's residuals is carried out using ordinary kriging, according to

$$\hat{\eta}(s_0) = \sum_{i=1}^{N} \lambda_i \eta(s_i) \qquad \text{with } \sum_{i=1}^{N} \lambda_i = 1, \tag{2.2}$$

where $\hat{\eta}(s_0)$ is the interpolated value at a point $s_o$, derived from the residuals of the linear regression model at the points of measurement $s_i$, $i = 1, \ldots, N$,

$\eta(s_i)$ are the residuals of the linear regr. model at $N$ points of measurement $s_i$, $i = 1, \ldots, N$,

$\lambda_1, \ldots, \lambda_N$ are the estimated weights based on the variogram, which is a measure of a spatial correlation, see Cressie (1993).

Prior to linear regression and interpolation, a logarithmic transformation on measurement and modelling data is applied based on the analysis presented in Guerreiro et al. (2015), as this contributes to a better fitting of the regression model and subsequent interpolation with the measurement and modelling data. After the interpolation, a back-transformation has to be performed.

Separate maps are created for the rural and the urban background areas on a grid at 10x10 km resolution. Subsequently, we merge the rural map and the urban background map into one combined air quality map using a weighting procedure based on the population density grid at 1x1 km resolution. For details, see Horálek et al. (2016). The final merged map on a 1x1 km resolution is used for exposure estimates. Exposure calculations have been proven to be more accurate when executing it on this higher resolution (Horálek et al., 2010). For presentational purposes of the European-wide map, we aggregate the 1x1 km grid resolution into a map at a 10x10 km grid resolution.

In our current mapping method, we apply at each area type a different combination of supplementary data, contributing to the best result. Based on the analysis presented in Guerreiro et al. (2015), chemical transport modelling output, altitude and wind speed are used for the rural areas, while for the urban background areas the supplementary data consist of chemical transport model (CTM) output and temperature.

At examining the variants on the current methodology, which are described in Sections 2.2 and 2.3, the selection of the supplementary data sources is re-evaluated on its improved fitting of the regression model and interpolation.

## 2.2 Pseudo BaP stations

For examining the potential of so-called *pseudo BaP data*, we use the methodology for $PM_{2.5}$ mapping as developed by Denby et al. (2011). We examine two different pseudo BaP data sources independent from each other: the first is a pseudo BaP dataset representing estimates of benzo(a)pyrene concentrations at $PM_{10}$ station locations without BaP measurement; the second, a pseudo BaP dataset representing BaP concentrations at $PM_{2.5}$ station locations without BaP measurement. These BaP estimates are based on the actual $PM_{10}$ resp. $PM_{2.5}$ measurement data and different supplementary data (like coordinates and meteorology), using multiple linear regression:

$$\hat{Z}_{BaP}(s) = c + b.Z_{PM}(s) + a_1.X_1(s) + \ldots + a_n.X_n(s) + \varepsilon(s) \tag{2.3}$$

where $\hat{Z}_{BaP}(\mathrm{s})$ is the estimated value of BaP at station *s*,

$Z_{PM}(\mathrm{s})$ is the measured value of $PM_{10}$ resp. $PM_{2.5}$ at station *s*,

$X_1(s), \ldots, X_n(s)$ are the values of other supplementary variables at station *s*,

$c, b, a_1, \ldots, a_n$ are the parameters of the linear regression model based on the data at the points of measurement stations with *both* BaP and $PM_{10}$ (resp. $PM_{2.5}$) measurements,

$n$ is the number of other supplementary variables used in the linear regression model (apart from $PM_{10}$ resp. $PM_{2.5}$).

Prior to linear regression, a logarithmic transformation on measurement data can be applied. In such case, a back-transformation of the estimated values has to be performed. Further, we examine both options, i.e. with and without the logarithmic transformation.

In this paper, we examine two variants of the pseudo BaP data, i.e. one based on $PM_{10}$ data and the other on $PM_{2.5}$ data. In line with the conclusion of Denby et al. (2011), we apply Eq. 2.3 for rural and urban/suburban background stations together.

For selection of the supplementary variables, the backward elimination is used (Horálek et al., 2007). The pseudo BaP data are subsequently used in the mapping as described in Equations 2.1 and 2.2.

## 2.3 Use of $PM_{2.5}$ rural and urban maps as supplementary data

As another alternative approach, we use the interpolated $PM_{2.5}$ rural and urban background maps as additional supplementary variables in the current BaP mapping method of Section 2.1. That means, next to the CTM-output, altitude and meteorological parameters used as supplementary data we now also include the interpolated rural resp. urban $PM_{2.5}$ background maps as additional supplementary data in the regression and interpolation. The separate $PM_{2.5}$ rural and urban background maps of 2013 that exist as intermediate products of the routinely $PM_{2.5}$ mapping (Horálek et al., 2015) are used. In this alternative approach the number of the stations used in Equation 2.2 is not enlarged, i.e. only the stations with BaP measurement data are considered.

## 2.4 Uncertainty estimates of the concentration maps

The uncertainty estimation of the concentration maps is on the one hand based on cross-validation and on the other hand based on the interpolation standard error map, calculated according to the principles of spatial statistics (Cressie, 1993).

The uncertainty estimation of the mapping results is based on the 'leave one out' *cross-validation* method. It computes the quality of the spatial interpolation for each measurement point from all available information except from the point in question, i.e. it withholds one data point and then makes a prediction at the spatial location of that point. This procedure is repeated for all measurement points in the available set. The results of the cross-validation are expressed by statistical indicators and scatter plots. The main indicators used are *root mean squared error* (RMSE) and *bias*:

$$RMSE = \sqrt{\frac{1}{N}\sum_{i=1}^{N}(\hat{Z}(s_i) - Z(s_i))^2} \quad (2.4)$$

$$Bias = \frac{1}{N}\sum_{i=1}^{N}(\hat{Z}(s_i) - Z(s_i)) \quad (2.5)$$

where $Z(s_i)$ is the observed air quality indicator value at the $i^{th}$ point,
$\hat{Z}(s_i)$ is the estimated air quality indicator value at the $i^{th}$ point using other information, except the observed indicator value at the $i^{th}$ point,
$N$ is the number of the observational points.

Next to the RMSE expressed in absolute units, one could express this uncertainty in relative terms by relating the RMSE to the mean of the air quality indicator value for all stations:

$$RRMSE = \frac{RMSE}{\frac{1}{N}\sum_{i=1}^{N}Z(s_i)}.100 \quad (2.6)$$

The *relative RMSE* (RRMSE) is expressed in percent.

Other cross-validation indicators are the coefficient of determination $R^2$ and the regression equation parameters *slope* and *intercept*, following from the scatter plot between the cross-validation predicted and the observed concentrations. All the cross-validation indicators are calculated based on the BaP measurement (not pseudo BaP) data.

The *standard error map* is calculated based on the spatial statistics theory, see Cressie (1993). The standard error of the combined (rural and urban background) map is calculated from the standard errors of the separate rural and urban background maps, as in De Smet et al. (2011). The relative standard error map is calculated by dividing the standard error by the concentration for each grid cell.

## 2.5 Uncertainty estimates of the pseudo BaP data

Uncertainty estimates of the pseudo BaP data are calculated in the points with both BaP and $PM_{10}$ measurements and with BaP and $PM_{2.5}$ measurements, respectively. The statistical indicators for the uncertainty analysis are *RMSE*, *bias*, $R^2$, *FAC50%* and *QO*. For all indicators, the pseudo BaP values estimated based on the multiple linear regression (Eq. 2.3) are related with the measurement BaP data.

*RMSE*, *bias*, and $R^2$ indicators are calculated according to Section 2.4. The two other statistical indicators are used likewise Denby et al. (2011):

- *FAC50%* shows the fraction of station predictions within ± 50% of the observed BaP values. This indicator is based on the uncertainty data quality objective for BaP measurements which is 50%, see Directive 2004/107/EC (EC, 2004). According to this Directive, 95% of the data is required to be within this range to fulfil the monitoring (fixed measurement) quality objective. This means that a *FAC50%* above 0.95 confirms fulfilment of just the monitoring quality objective for the pseudo BaP data.

- *QO* shows the fraction of station predictions that fulfil the monitoring/assessment Quality Objective according to the Directive. We present this indicator in two variants as *QO1* and *QO2*. This indicator is calculated in the same way as FAC50% for observed BaP values above the lower assessment threshold (LAT) for BaP (0.4 $ng.m^{-3}$), i.e. the allowable error of predictions is 50% in these cases. For observed BaP values being below or equal to the LAT, the predictions are accounted as fulfilling based on the data quality objective of the Directive for modelling (in the case of *QO1*) or for objective estimation (in the case of *QO2*). For modelling the allowable error is 60 % and for objective estimation it is 100 %. The reason for this choice is that monitoring is not mandatory for areas where the levels are below the LAT and modelling or objective estimation techniques can be used as the sole ways of assessment. As such, the *QO1* and *QO2* indicators give a more complete overview of meeting the full set of data quality objectives for BaP as laid down in the Directive.

# 3 Input data

The mapping method is based on air quality measurements and in two alternatives explored to support, with the use of additional pseudo data from PM measurements. These point data are described in Sections 3.1 and 3.2.

Furthermore, we apply *gridded* chemical transport model results (Section 3.3) and other *gridded* supplementary data, such as altitude and meteorology (Section 3.4) and routine $PM_{2.5}$ mapping products (Section 3.5). Before the execution of a linear regression model, followed by its residuals kriging, we convert all gridded input data into the EEA reference projection ETRS89-LAEA5210 on a 10x10 km grid resolution.

The *gridded* population data (Section 3.4), however, was converted into the EEA reference projection on a 1x1 km resolution. It allows us to do the weighted merging of the rural and the urban background maps into the final map and its subsequent exposure calculations more accurately than on the 10x10 km resolution, see Section 2.1.

For details of the supplementary data and its aggregation, see Horálek et al. (2007 and 2016).

## *3.1 Benzo(a)pyrene monitoring data*

Air quality monitoring data for 2013 were extracted from the Air Quality e-Reporting database, EEA (2015). Only data from stations classified as background for the areas rural, suburban and urban are used. Industrial and traffic station types are not considered, as they represent local scale concentration levels not applicable at the mapping resolution employed. In agreement with Guerreiro et al. (2015), the following indicators of BaP concentrations in ambient air (with the e-reporting component number, cp_number) were extracted:

Benzo(a)pyrene, 2013 annual average (ng.m$^{-3}$)
– BaP in $PM_{2.5}$, aerosol (cp_number = 1029)
– BaP in $PM_{10}$, aerosol (cp_number = 5029)
– BaP in $PM_{10}$, air+aerosol (cp_number = 5129)
– BaP, air+aerosol (cp_number = 6015)

The actual given BaP concentration values as extracted from the AQ e-reporting database were taken. Despite the fact that the European directive (EC, 2004) prescribes that the BaP concentration measurements should be made in the $PM_{10}$ fraction, available data for all the species listed above are considered in this paper. The justification for this is that most of the BaP is present in $PM_{2.5}$ and not in the coarser fraction of $PM_{10}$, and the gaseous fraction of the total BaP is quite small (Guerreiro et al., 2015).

Only the stations inside the EEA map extent Map_1c (EEA, 2011) are used. To reach a more extended spatial coverage, the e-reporting data set was supplemented with additional data provided by SHMI and EEA, i.e. by several Slovak and Italian stations, see Annex I.

Measurements from stations with data coverage of at least 14 percent valid measurements per year were used in order to maximise the use of the available measurement data, which are already scarce in large areas of Europe. A data coverage of 14% corresponds to the minimum time coverage for indicative measurements laid down in Directive 2004/107/EC (EC, 2004). The sampling should be spread evenly over the year, in order to secure that the annual average calculated from the available data is representative of the real value. Two stations with greatest deviation in the data sampling distribution were excluded, namely the Spanish stations ES0006R and ES0007R.

Map 3.1 shows the rural and urban/suburban background measurement stations used for BaP mapping. Together with the geographical distribution of the stations, the map illustrates also the measurement concentration levels. In total, 77 rural background and 296 urban/suburban background stations were used.

**Map 3.1 Measurement air quality data from rural (left) and urban/suburban (right) background stations. BaP, annual average, 2013. Units: ng.m$^{-3}$.**

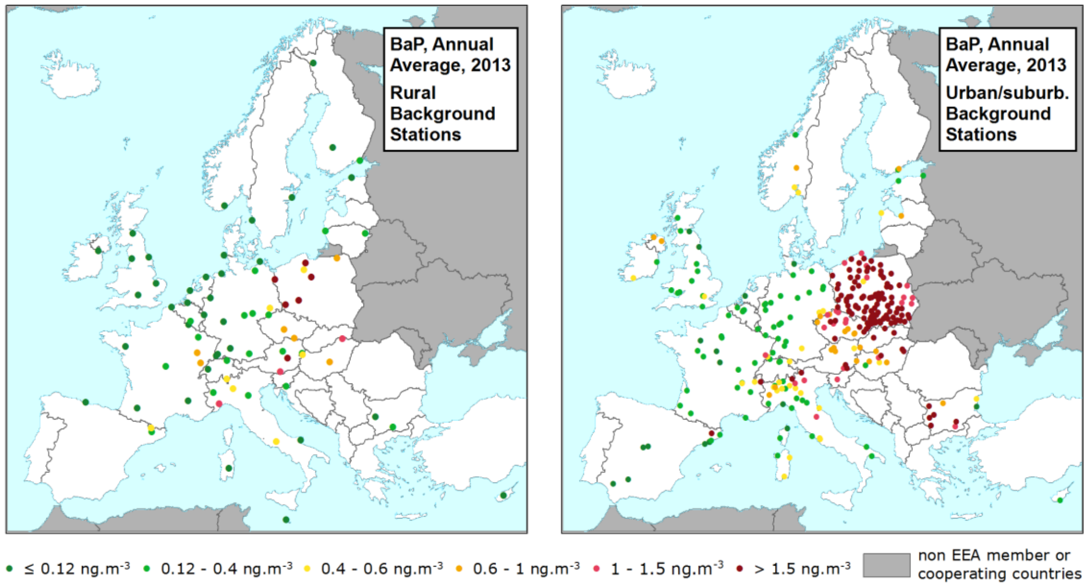


## 3.2 *$PM_{10}$ and $PM_{2.5}$ monitoring data*

$PM_{10}$ and $PM_{2.5}$ monitoring data are extracted from the Air Quality e-Reporting database, EEA (2015). The set was supplemented with 30 Italian urban/suburban background stations submitted to the Air Quality e-Reporting database after the publishing of the 2013 data set (see Annex 1) and with several rural stations from the database EBAS (NILU, 2015) not reported to the Air Quality e-Reporting database. Only data from stations classified by the Air Quality e-Reporting database and/or EBAS of the type *background* for the area types *rural*, *suburban* and *urban* are selected. The following substances and their indicators are extracted:

$PM_{10}$ – annual average [µg.m$^{-3}$], year 2013
$PM_{2.5}$ – annual average [µg.m$^{-3}$], year 2013

Only the stations with annual data coverage of at least 75 percent are selected.

In the case of $PM_{10}$, it resulted in a set of 311 rural background and 1007 urban/suburban background stations; for $PM_{2.5}$, the set consists of 147 rural background and 454 urban/suburban background stations.

Out of all the considered $PM_{10}$ stations, 60 rural and 234 urban/suburban background stations are collocated with the BaP stations. For $PM_{2.5}$ stations, it is 36 rural and 126 urban/suburban background stations.

## 3.3 *Chemical transport modelling BaP data*

The chemical dispersion model used is the *EMEP MSC-E POP* model, EMEP (2016a). It is a three-dimensional Eulerian multi-compartment chemistry transport model (Gusev et al., 2005, 2006). Its resolution is circa 50x50 km. The model's output covers completely the mapping domain (i.e. the area of the EEA member and cooperating countries within the map extent Map_1c, EEA, 2011). The parameter used is

Benzo(a)pyrene – annual average [ng.m$^{-3}$], year 2013

Map 3.2 presents the modelled BaP annual average concentrations for 2013. The modelled concentrations were obtained on the basis of 2013 emissions and 2013 meteorology. For details on the emission used, see EMEP (2016b).

It should be noted that the model is highly sensitive to the emission year accounted for. To illustrate this, we present in Annex 2 the model output for BaP annual average for 2013, but based on 2012 emissions and 2013 meteorology (EMEP, 2015), see Map A2.1. The difference between Map 3.2 and A2.1 is solely caused by the differences in emissions for 2012 and 2013 and is illustrative for the high variability in emission data from one year to another.

Under the LRTAP Convention, parties are required to report emission data for PAHs and BaP, among other pollutants. Never the less, not all countries report their emissions. Those who do report may only report for one/few emission sectors and not necessarily the most important sector. For modelling purposes, EMEP estimates BaP emissions for their European modelling domain, but given the poor emission reporting in several countries, there are very large uncertainties in the estimated emissions. The variability in emissions from year to year in some countries is an indicator of this uncertainty.

**Map 3.2 Output of EMEP chemical transport model. BaP annual average in 2013. Units: ng.m$^{-3}$.**

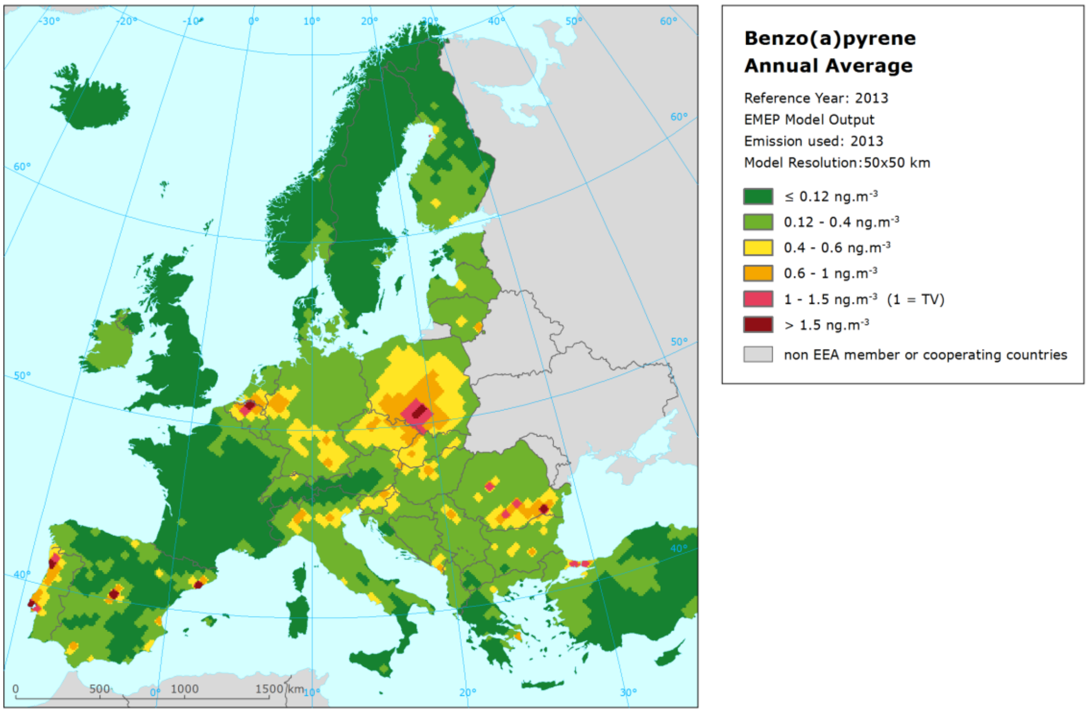


## *3.4 Altitude, meteorological data, population density*

The *altitude* data field (in m) with an original grid resolution of 15x15 arcseconds is taken from GTOPO30 ([https://lta.cr.usgs.gov/GTOPO30](https://lta.cr.usgs.gov/GTOPO30)).

The *meteorological parameters* used are *wind speed* (annual average for 2013, in m.s$^{-1}$), *surface net solar radiation* (annual average of daily sum for 2013, MWs.m$^{-2}$) and *temperature* (annual average for

2013, °C). The daily data in resolution 15x15 arc-seconds were extracted from the Meteorological Archival and Retrieval System (MARS) of ECMWF, see ECMWF (2015).

*Population density* (in inhabitants.$km^{-2}$, census 2011) is based on Geostat 2011 grid dataset (Eurostat, 2014). The dataset is in 1x1 km resolution, in the EEA reference grid. For regions not included in the Geostat 2011 dataset we use as alternative sources JRC (2009) and ORNL (2008) data. For details, see Horálek et al. (2016).

### 3.5 Interpolated $PM_{2.5}$ rural and urban background maps

As another alternative, the interpolated $PM_{2.5}$ rural and urban background maps as prepared under Horálek et al. (2016) are used as additional supplementary variables. The maps are in 10x10 km resolution, and represent

$PM_{2.5}$ – annual average [$\mu g.m^{-3}$], year 2013, rural map
$PM_{2.5}$ – annual average [$\mu g.m^{-3}$], year 2013, urban background map

For details, see Horálek et al. (2016).

# 4 Analysis

This chapter investigates the suitability of the pseudo stations data approach and examines potential improvements of the benzo(a)pyrene mapping.

Section 4.1 describes and examines the two sets of pseudo BaP station data derived from existing $PM_{10}$ resp. $PM_{2.5}$ station data based on the multiple linear regression. Before doing this, we first selected the optimal set of supplementary data. Next to this, we checked the usefulness of the logarithmic transformation in the calculations.

In Section 4.2, the two sets of pseudo BaP station data are – together with available observed BaP data – used in the mapping. These maps are compared with the maps created based on the current methodology and on the alternative approach utilizing the $PM_{2.5}$ rural and urban background maps.

## 4.1 Pseudo BaP stations analysis

As described in Section 2.2, multiple linear regression (MLR) of the observed BaP concentrations with the observed $PM_{10}$ or $PM_{2.5}$ concentrations and other supplementary data is carried out to produce pseudo BaP stations. Two variants of the multiple linear regression were considered, i.e. without and with the logarithmic transformation of the observed BaP and $PM_{10}$ resp. $PM_{2.5}$ data. First, the suitable supplementary data were selected. The supplementary data tested included latitude, longitude, altitude, wind speed, temperature, surface net solar radiation and population. The latitude and longitude are included in the station data. Altitude is available from two sources: in the station point data and as gridded GTOPO30 dataset. The rural and urban/suburban background stations are handled together.

For both $PM_{10}$ and $PM_{2.5}$ variants without logarithmic transformation, the supplementary data selected as most optimal are latitude, GTOPO30 altitude and wind speed. For the variants with logarithmic transformation, the supplementary data selected are longitude and surface solar radiation for $PM_{10}$, resp. longitude and latitude for $PM_{2.5}$. Table 4.1 presents the relevant parameters and statistical indicators.

**Table 4.1 Parameters of the multiple linear regression (Eq. 2.3) and its statistics for generation of pseudo BaP station data based on $PM_{10}$ (left) and $PM_{2.5}$ (right) data, for BaP 2013 annual average.**

| multiple linear regression | $PM_{10}$ variant | | $PM_{2.5}$ variant | |
|---|---|---|---|---|
| | without log. tr. | with log. tr. | without log. tr. | with log. tr. |
| | coeff. | coeff. | coeff. | coeff. |
| c (constant) | -15.67 | -5.87 | -11.12 | -13.37 |
| b ($PM_{10}$ measured data, 2013 annual average) | 0.228 | 2.439 | | |
| b ($PM_{2.5}$ measured data, 2013 annual average) | | | 0.257 | 2.586 |
| a1 (latitude) | 0.191 | | 0.102 | 0.102 |
| a2 (longitude) | | 0.059 | | 0.044 |
| a3 (altitude GTOPO) | 0.0030 | | 0.0024 | |
| a4 (wind speed, annual average 2013) | 0.427 | | 0.715 | |
| a5 (surface solar radiation, annual sum 2013) | | -0.305 | | |
| **N of stations** | 294 | 294 | 162 | 162 |
| **adjusted $R^2$** | **0.723** | **0.776** | **0.690** | **0.774** |
| **standard error [$ng.m^{-3}$]** | **1.49** | **0.76** | **1.26** | **0.73** |

Based on the parameters presented in Table 4.1, we calculated the pseudo BaP data. It should be noted that for the variant without the logarithmic transformation, in some cases the estimated pseudo BaP value is negative. In such cases, this negative value is substituted by the value 0.005 $ng.m^{-3}$ (as a supposed lowest level of the detection limit across the measurement devices used in the national networks). Table 4.2 presents the uncertainty estimates of the pseudo BaP data, performed separately for the rural and urban background areas.

**Table 4.2 Uncertainty estimates of the pseudo BaP station data based on $PM_{10}$ or $PM_{2.5}$ data for BaP 2013 annual average.**

| pseudo data variant | rural areas | | | | | | | |
|---|---|---|---|---|---|---|---|---|
| | N | RMSE | bias | $R^2$ | regr. eq. | FAC50% | QO1 | QO2 |
| $PM_{10}$ data, without logarithmical transformation | 60 | 0.63 | 0.19 | 0.26 | y=0.644x+0.32 | 0.17 | 0.17 | 0.52 |
| $PM_{10}$ data, with logarithmical transformation | 60 | 0.37 | -0.01 | 0.49 | y=0.515x+0.18 | 0.52 | 0.55 | 0.63 |
| $PM_{2.5}$ data, without logarithmical transformation | 36 | 0.62 | 0.27 | 0.30 | y=1.059x+0.26 | 0.14 | 0.14 | 0.58 |
| $PM_{2.5}$ data, with logarithmical transformation | 36 | 0.30 | 0.07 | 0.41 | y=0.646x+0.15 | 0.39 | 0.42 | 0.61 |
| | | | | | | | | |
| pseudo data variant | urban background areas | | | | | | | |
| | N | RMSE | bias | $R^2$ | regr. eq. | FAC50% | QO1 | QO2 |
| $PM_{10}$ data, without logarithmical transformation | 234 | 1.54 | 0.12 | 0.75 | y=0.664x+0.99 | 0.50 | 0.50 | 0.63 |
| $PM_{10}$ data, with logarithmical transformation | 234 | 1.47 | -0.44 | 0.79 | y=0.685x+0.38 | 0.67 | 0.68 | 0.74 |
| $PM_{2.5}$ data, without logarithmical transformation | 126 | 1.29 | 0.09 | 0.73 | y=0.638x+0.77 | 0.37 | 0.37 | 0.52 |
| $PM_{2.5}$ data, with logarithmical transformation | 126 | 1.32 | -0.45 | 0.79 | y=0.588x+0.33 | 0.63 | 0.66 | 0.69 |

Next to the commonly used statistical indicators $R^2$, *RMSE* and *bias*, three other indicators are included: *FAC50%, QO1* and *QO2*, see Section 2.5.

It should be noted that results for the variants based on $PM_{10}$ are not directly comparable with the variants based on $PM_{2.5}$, due to the different sets of the stations used.

Comparing the variants without and with the use of the logarithmic transformation, the similar findings can be stated for both $PM_{10}$ and $PM_{2.5}$ data variants. In the rural areas, the variant with the logarithmic transformation gives considerably better results for all the observed statistics. In the urban areas, the use of the logarithmic transformation gives better results for FAC50%, Q1 and QO2, slightly better or similar results for *RMSE* and $R^2$, but worse results for *bias*. Looking more deeply into the bias, we found that the results are influenced by extremely high concentration values at the Polish urban/suburban background stations, for which the pseudo BaP stations give underestimated results. If we remove all Polish urban/suburban background pseudo BaP stations, there would be no bias for the variant with the logarithmic transformation (both for pseudo stations based on $PM_{10}$ and $PM_{2.5}$), while for the variant without the logarithmic transformation there is considerable bias (i.e. 0.4 $ng.m^{-3}$, resp. 0.5 $ng.m^{-3}$ for the pseudo stations based on $PM_{10}$ resp. $PM_{2.5}$). It can be concluded that the pseudo stations data calculated with the use of the logarithmic transformation give better results. Next to this, it is recommended not to use the Polish urban/suburban background pseudo stations due to their underestimated values and due to the fact there is enough BaP urban measurements in Poland. (In 2013, out of the 296 urban/suburban background stations with enough BaP data, just 105 were located in Poland.)

Based on the variants without and with the use of the logarithmic transformation, we further use just the variant with the logarithmic transformation. The variant without the logarithmic transformation is not further considered in the paper.

One can see that the fraction of the "satisfactory" predictions (*QO2*) is 0.63 resp. 0.74 (for the rural resp. urban areas) for the $PM_{10}$ variant and 0.61 resp. 0.69 for the $PM_{2.5}$ variant. It should be noted these numbers are quite low compared to 0.95 required by the EC Directive (EC, 2004) for monitoring, even if the allowable error for values below LAT is much bigger (100 % vs. 50 %), see Section 2.5.

Figure 4.1 shows the scatter plots of the pseudo BaP annual averages against the measurement BaP annual averages. The area between the two continuous lines represents the area where the predictions are within ± 50% of the observed BaP data, i.e. the FAC50% area. It can be seen that the predicted values for the concentrations above 5 $ng.m^{-3}$ are in general underestimated, although mostly within the FAC50% area. It should be noted that all such extremely high values were measured at the Polish urban/suburban background stations.

**Figure 4.1 Scatter plots of the pseudo BaP data using $PM_{10}$ (top) and $PM_{2.5}$ (bottom) data against measured BaP data for rural (left) and urban background (right) areas. Logarithmic transformation is used in the pseudo data calculations. Annual average, 2013. Units: $ng.m^{-3}$.**

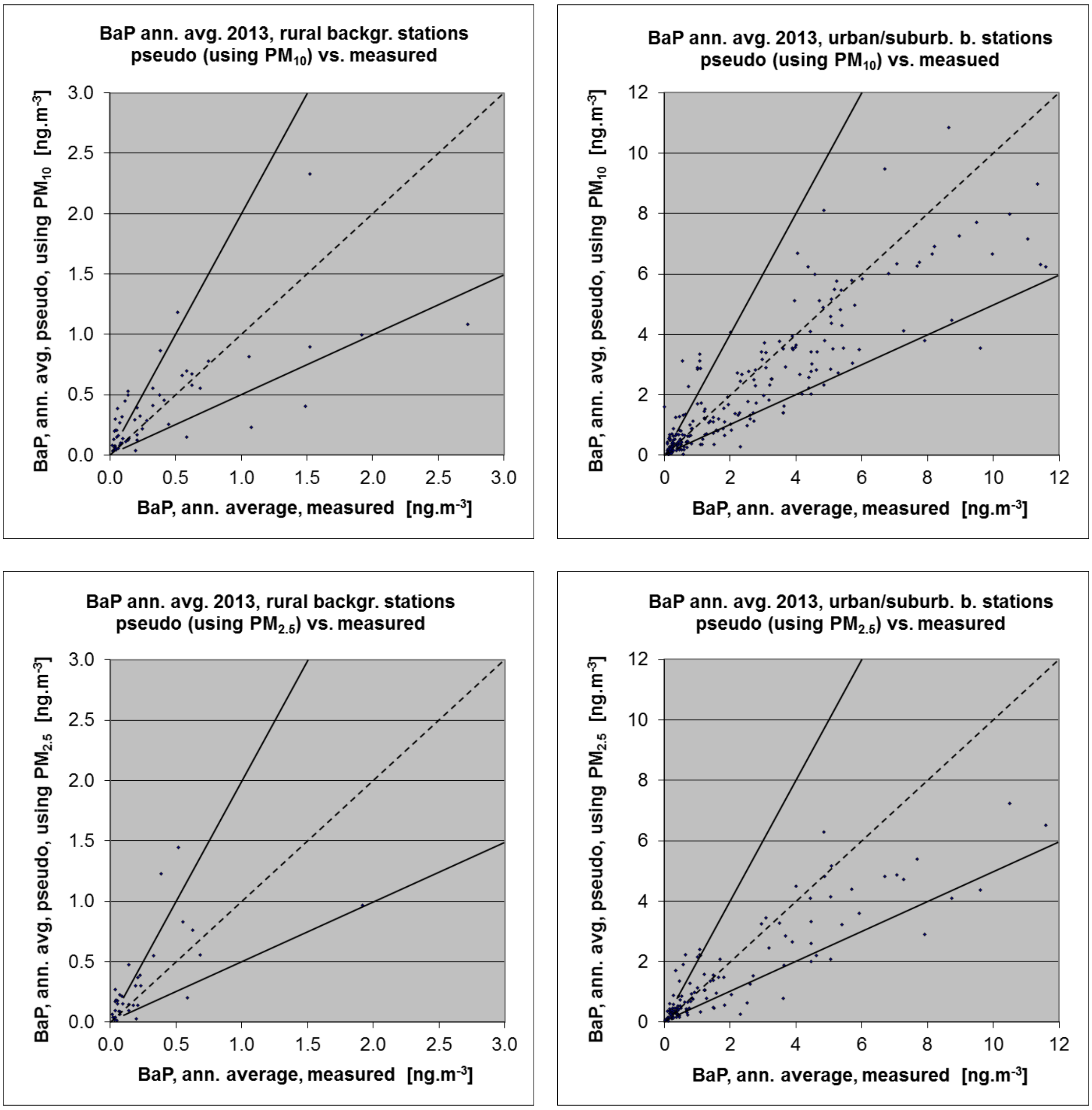


Based on the multiple linear regression presented in Table 4.1, the BaP concentration were estimated in the points of $PM_{10}$ and $PM_{2.5}$ stations. Map 4.1 presents the geographical distribution of these pseudo BaP stations based on existing $PM_{10}$ monitoring stations, including their relevant estimated BaP concentration levels. Map 4.2 presents the same for the pseudo BaP stations based on existing $PM_{2.5}$ monitoring stations. Note that these maps represent only station points where no BaP measurements take place.

Comparing Maps 4.1 and 4.2 with Map 3.1, no considerable differences are found. In some areas such as the Benelux and the eastern Germany, the actual BaP measurement stations show slightly lower BaP values compared to the pseudo stations estimates.

**Map 4.1 Pseudo BaP data based on $PM_{10}$ for rural (left) and urban/suburban (right) background stations. Logarithmic transformation is used in the pseudo data calculations. BaP, annual average, 2013. Units: $ng.m^{-3}$.**

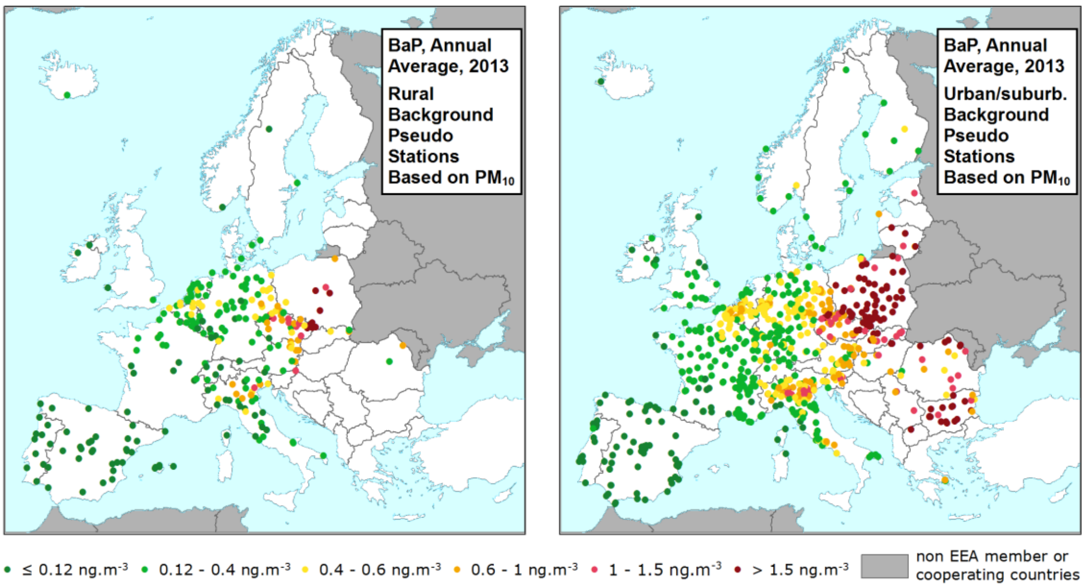


**Map 4.2 Pseudo BaP data based on $PM_{2.5}$ for rural (left) and urban/suburban (right) background stations. Logarithmic transformation is used in the pseudo data calculations. BaP, annual average, 2013. Units: $ng.m^{-3}$.**

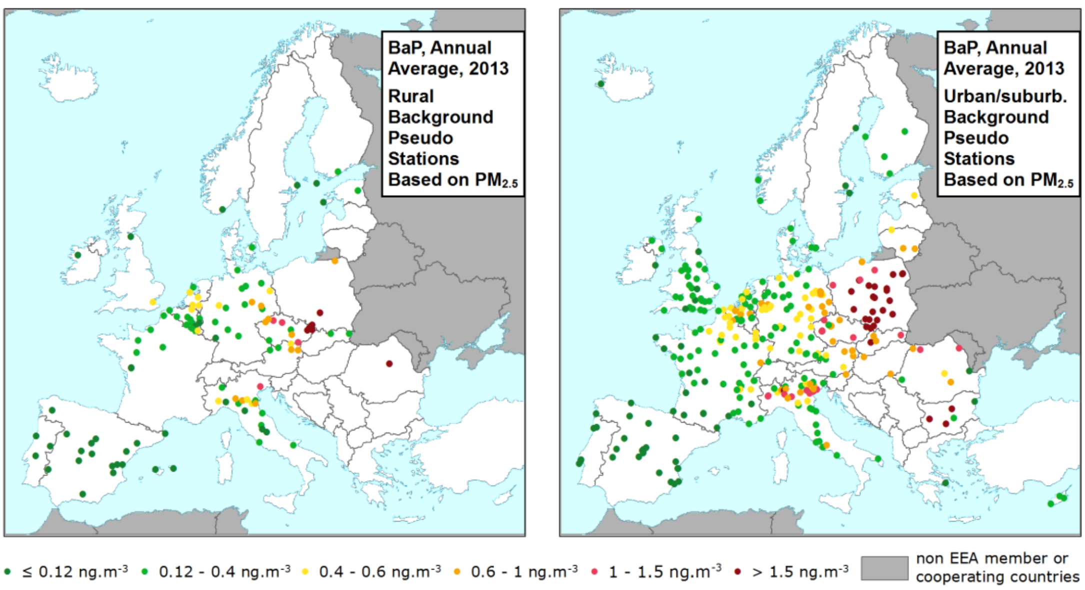

Both the two pseudo BaP stations data sets are further used in Section 4.2, in which we examine and compare different mapping methods, with the emphasis on the comparison of the two pseudo BaP stations methods in the mapping analysis with the other alternatives. We suppose the use of these pseudo BaP data sets as potential beneficial, even though they do not satisfy the requirement of the EC Directive (EC, 2004) for monitoring, see above.

In agreement with the recommendation of the pseudo BaP stations analysis, the urban/suburban pseudo BaP stations located in Poland (as can be seen in the right figures in Maps 4.1 and 4.2) are not included in the pseudo BaP data sets. In total, 962 (i.e. 251 rural and 711 urban/suburban) pseudo BaP stations based on $PM_{10}$ and 415 (i.e. 112 rural and 303 urban/suburban pseudo BaP stations based on $PM_{2.5}$ are further used in Section 4.2.

## *4.2 Comparison of mapping methods*

In this section, we compare current mapping method with the three alternative BaP mapping methods. The methods are

(i) current method (i.e. the method presented in Guerreiro et al. (2015)
(ii) mapping using pseudo BaP stations based on $PM_{10}$
(iii) mapping using pseudo BaP stations based on $PM_{2.5}$
(iv) mapping using $PM_{2.5}$ rural and urban maps.

The map using (i) current method is prepared as described in Section 2.1, based on the BaP observational data (Section 3.1) and the supplementary data as presented in Guerreiro et al. (2015), i.e. EMEP model output, altitude and wind speed for the rural areas and EMEP model output and temperature for the urban/suburban areas.

The maps using (ii) pseudo BaP stations based on $PM_{10}$ and (iii) pseudo BaP stations based on $PM_{2.5}$ are prepared using the same method of linear regression model followed by kriging of its residuals as under (i), but now based on both observational and pseudo BaP station data. The pseudo BaP station data are the estimates of Section 4.1 based on $PM_{10}$ resp. $PM_{2.5}$ stations calculated with the use of the logarithmic transformation. For selecting the optimal set of the supplementary data, the backward regression elimination analysis was applied, alike Horálek et al. (2007) and Guerreiro et al. (2015). This led to the selection of EMEP modelling data, altitude, surface solar radiation and wind speed for the rural areas, resp. EMEP model output, surface solar radiation and wind speed for the urban areas, for both (ii) and (iii) methods.

Additionally, another alternative approach to create a BaP interpolated map is included in the comparison. It is method number (iv): an interpolated BaP map based on the use of the separate rural map and urban interpolated map for $PM_{2.5}$ (Section 2.3) as additional supplementary data source in the current method of Section 2.1. This interpolated BaP map is prepared on basis of the same set of BaP observational data as applied in method (i). Again, by the backward regression elimination we selected the other useful supplementary data for deriving the most optimal regression model. For the regression model of the rural areas, we selected the EMEP modelling data and wind speed, while for regression model of the urban areas it was the EMEP modelling data only.

For all methods we applied in addition a logarithmic transformation on the measurement and EMEP modelling data in the process of preparing the rural and urban maps that are ultimately merged into a final map for BaP.

The statistical parameters for both the rural and the urban interpolation results of the four methods are presented in Table 4.3.

**Table 4.3 Parameters of the linear regression models and of the ordinary kriging variograms (nugget, sill, range) of BaP annual average for 2013 in rural and urban areas for each of the four methods (i) – (iv).**

| linear regr. model + OK of its residuals | (i) current | | (ii) pseudo from $PM_{10}$ | | (iii) pseudo from $PM_{2.5}$ | | (iv) using $PM_{2.5}$ | |
|---|---|---|---|---|---|---|---|---|
| | rural | urban | rural | urban | rural | urban | rural | urban |
| | coeff. | coeff. | coeff. | coeff. | coeff. | coeff. | coeff. | coeff. |
| c (constant) | 1.38 | 2.99 | 4.79 | 4.78 | 4.27 | 4.76 | -3.85 | -8.25 |
| a1 (ln EMEP model) | 0.585 | 0.637 | 0.538 | 0.429 | 0.522 | 0.392 | 0.293 | 0.139 |
| a2 (altitude GTOPO) | -0.00099 | | -0.00160 | | -0.00117 | | | |
| a3 (wind speed) | -0.480 | | -0.461 | -0.341 | -0.493 | -0.361 | -0.248 | |
| a4 (temperature) | | -0.244 | | | | | | |
| a5 (s. solar rad.) | | | -0.342 | -0.366 | -0.296 | -0.354 | | |
| a6 (ln $PM_{2.5}$ rur. map) | | | | | | | 1.483 | |
| a7 (ln $PM_{2.5}$ urb. map) | | | | | | | | 2.860 |
| **N of stations** | 77 | 296 | 328 | 1007 | 189 | 599 | 77 | 296 |
| **adjusted $R^2$** | **0.31** | **0.39** | **0.59** | **0.44** | **0.48** | **0.39** | **0.42** | **0.53** |
| **st. err. [μg.m$^{-3}$]** | **1.10** | **1.15** | **0.96** | **0.99** | **1.09** | **1.11** | **1.01** | **1.01** |
| nugget | 0.38 | 0.03 | 0.31 | 0.13 | 0.24 | 0.19 | 0.39 | 0.01 |
| sill | 1.81 | 0.62 | 0.87 | 0.74 | 1.34 | 0.81 | 1.41 | 0.43 |
| range [km] | 940 | 250 | 950 | 910 | 950 | 690 | 940 | 200 |

All four methods were mutually compared by means of the 'leave one out' cross-validation (Section 2.4). The comparison results are presented in Table 4.4. The cross-validation indicator values are calculated based on the BaP monitoring data only (i.e. not using the pseudo BaP data). Thus, the results of the different methods are mutually comparable. The best results are marked by dark green, the second best by light green.

**Table 4.4 Comparison of different methods of spatial interpolation showing RMSE, RRMSE, bias, $R^2$ and linear regression from the cross-validation scatter plots of BaP annual mean predicted values, 2013. Units: ng.m$^{-3}$ except RRMSE and $R^2$.**

| | spatial interpolation variant + supplementary data used | rural areas | | | | |
|---|---|---|---|---|---|---|
| | | RMSE | RRMSE | bias | $R^2$ | regr. eq. |
| (i) | **current method (EMEP, altitude, wind speed)** | 0.57 | 146.4% | 0.08 | 0.18 | y=0.389x+0.32 |
| (ii) | **using pseudo stations from $PM_{10}$ (EMEP, alt., w. sp, s.s. rad.)** | 0.47 | 122.3% | -0.01 | 0.28 | y=0.383x+0.23 |
| (iii) | **using pseudo stations from $PM_{2.5}$ (EMEP, alt., w. sp., s.s. rad.)** | 0.48 | 123.0% | 0.04 | 0.33 | y=0.495x+0.23 |
| (iv) | **using $PM_{2.5}$ rural map (EMEP, w. sp., $PM_{2.5}$ rural map)** | 0.50 | 129.9% | 0.07 | 0.32 | y=0.529x+0.25 |
| | | | | | | |
| | spatial interpolation variant + supplementary data used | urban background areas | | | | |
| | | RMSE | RRMSE | bias | $R^2$ | regr. eq. |
| (i) | **current method (EMEP, temperature)** | 1.46 | 65.2% | -0.01 | 0.74 | y=0.758x+0.53 |
| (ii) | **using pseudo stations from $PM_{10}$ (EMEP, s. s. rad., w. speed)** | 1.54 | 69.0% | -0.16 | 0.71 | y=0.682x+0.55 |
| (iii) | **using pseudo stations from $PM_{2.5}$ (EMEP, s. s. rad., w. speed)** | 1.51 | 67.6% | -0.05 | 0.72 | y=0.719x+0.58 |
| (iv) | **using $PM_{2.5}$ urban backgr. map (EMEP, $PM_{2.5}$ urban b. map)** | 1.37 | 61.4% | -0.03 | 0.77 | y=0.784x+0.45 |

It can be seen that the map using (iii) pseudo stations based on $PM_{2.5}$ observations gives slightly better results than the map using (ii) pseudo stations based on $PM_{10}$ observations. Both the two pseudo stations methods provide better results compared to the level of the (i) current mapping method in the rural areas, while the results of (i) in the urban areas are slightly better compared to (ii) and (iii) results. The best results for urban areas are given by the method (iv) using $PM_{2.5}$ urban background maps. For rural areas, the method (iv) gives quite similar results like (ii) and (iii). Nevertheless, it should be noted that the double use of the wind speed as a supplementary variable in the method (iv) for the rural areas (both in the $PM_{2.5}$ and BaP mapping) may lead to slight deviation of the map. For future, this shortcoming could be possibly eliminated by the removing of wind speed from the supplementary variables used in the BaP mapping.

The bias detected in the urban areas for method (ii) is limited mainly to Poland. It is influenced by the low slope of the regression equation and the extremely high concentrations at Polish stations in urban areas. If the statistics are calculated without Polish stations, no bias is detected. While the measured BaP annual mean averaged across all the Polish urban and suburban background stations is at the level of 5.0 $ng.m^{-3}$, the relevant value estimated under the method (ii) is underestimated of about 10%.

For all four methods, the rural and urban maps are ultimately merged into a final map of BaP using the population density grid as described in Section 2.1. Next to the concentration maps, the uncertainty map showing the interpolation relative standard error has been constructed. The acceptable relative standard error is below 0.60 (see Directive EC 2004/107/EC, Annex IV, objectives for modelling).

Map 4.3 presents the final merged map created with the (i) current methodology, being our point of departure in the improvement exploration, and the relative standard error for this concentration map. Maps 4.4 and 4.5 show the final merged maps created with methods using (ii) pseudo stations based on $PM_{10}$ and (iii) pseudo stations based on $PM_{2.5}$, and the relative standard error of these maps. Map 4.6 presents the final merged maps created by method (iv) using the maps of $PM_{2.5}$ for rural areas and urban areas as additional supplementary data, as well as the relative standard error of this map.

Comparing the relative standard error maps one can see that the best results are given by method (ii), the second best results are shown by method (iii). The main reason is in the number of the stations: the use of the pseudo stations in the interpolation decreases the interpolation error. However, it should be noted that the relative standard error of methods (ii) and (iii) is maybe somewhat underestimated, particularly in the areas with the lack of BaP measurements, as the pseudo BaP stations do not satisfy the requirement of the EC Directive for monitoring, see Section 4.1.

Limiting the BaP concentration maps for 2013 to the areas with acceptable relative standard error below 0.60 (see above), we obtain the concentration maps presented in Maps 4.7 and 4.8. In these final maps, we present the results of methods (i) – (iv).

The current method (i) shows smaller area with the acceptable uncertainty compared to the similar map for 2012, see Guerreiro et al. (2015). The main reason is in overall lower BaP concentrations in 2013 compared to 2012, leading to higher relative uncertainty.

The method (ii) using pseudo stations based on $PM_{10}$ shows the largest area with the acceptable uncertainty, while the method (iv) using $PM_{2.5}$ rural and urban background maps shows the best cross-validation results in Table 4.4. The method (iii) using pseudo stations based on $PM_{2.5}$ shows the second largest area with the acceptable uncertainty and the second best cross-validation results.

Taking into account both the cross-validation and the relative standard error results, the most promising – for the time being with the lack of the BaP stations – seems to be the method (iii) using pseudo stations based on $PM_{2.5}$. Furthermore, this method could be potentially improved by including the pseudo $PM_{2.5}$ stations (Horálek et al., 2016), which would increase the number of pseudo BaP stations based on $PM_{2.5}$.

**Map 4.3** **Spatial interpolated concentration field of annual mean BaP in 2013, created by (i) current methodology (top) and uncertainty map showing interpolation relative standard error for this map (bottom). Units: ng.m$^{-3}$.**

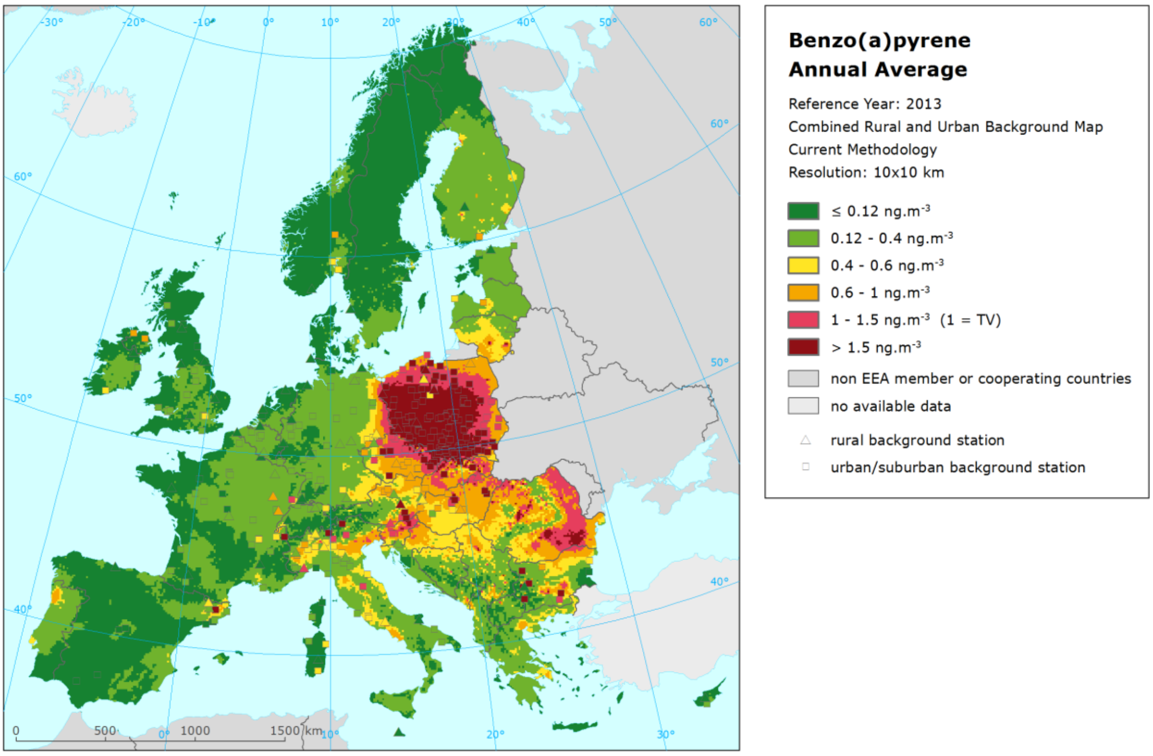


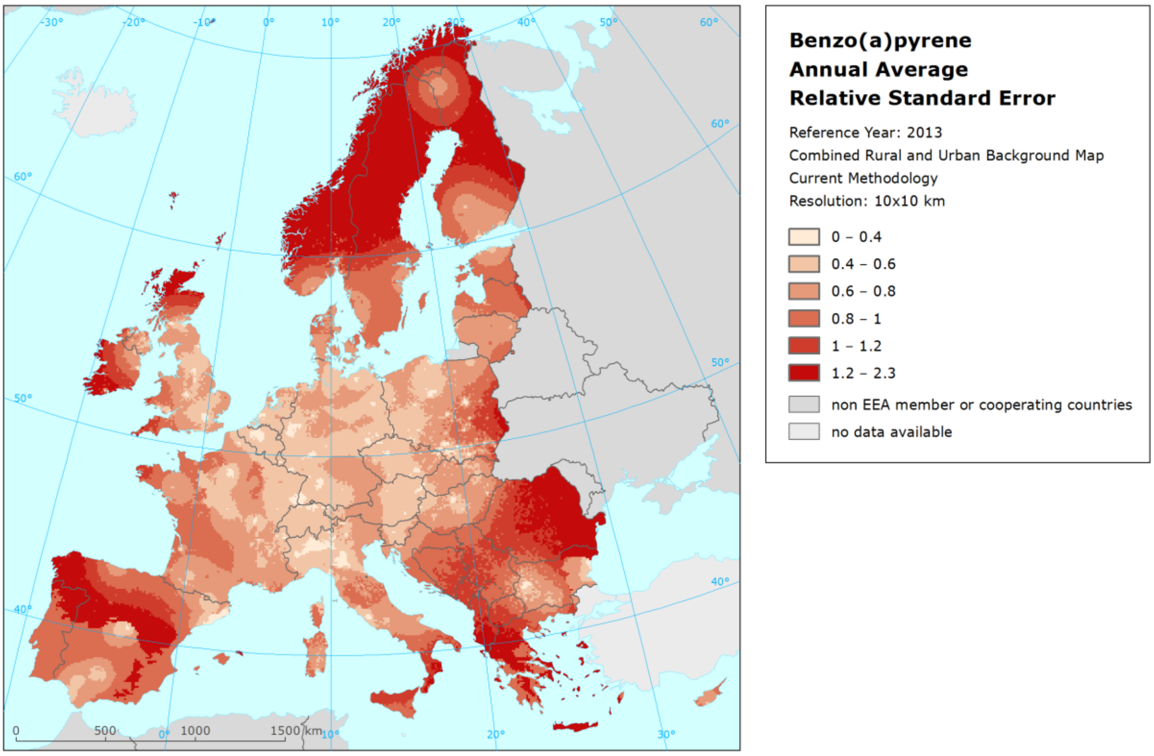

**Map 4.4** **Spatial interpolated concentration field of annual mean BaP in 2013, created using (ii) pseudo stations based on $PM_{10}$ (top) and uncertainty map showing relative standard error for this map (bottom). Units: ng.m$^{-3}$.**

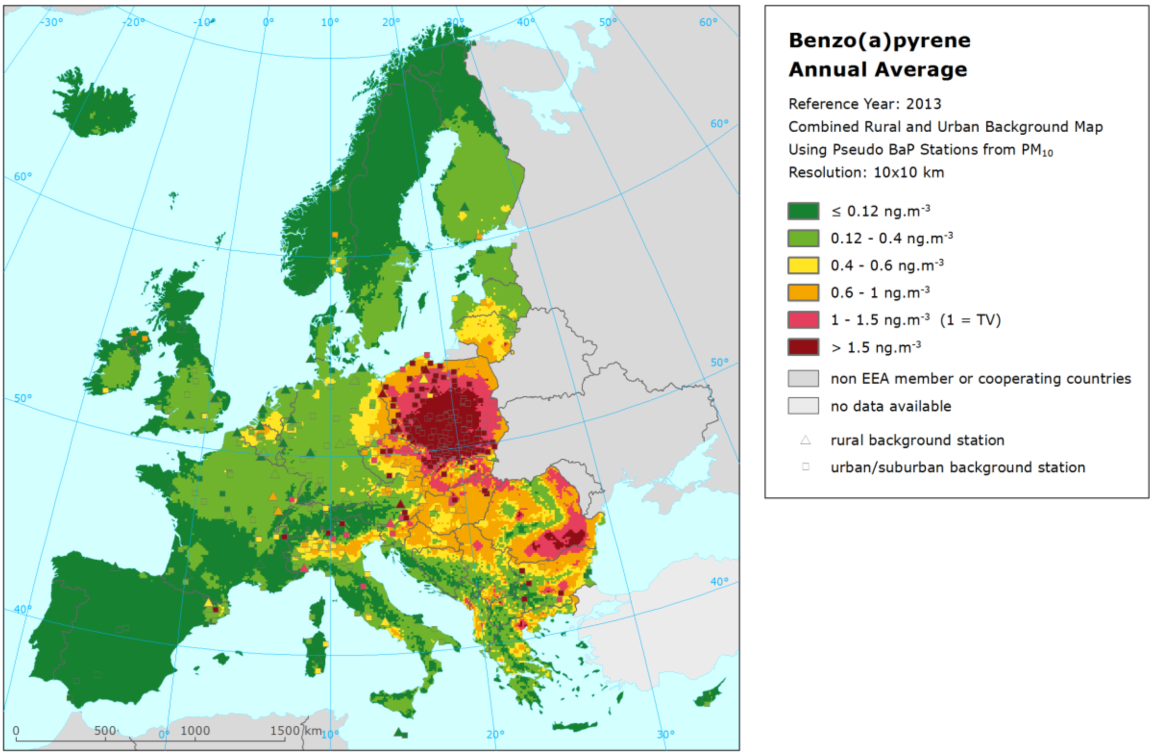


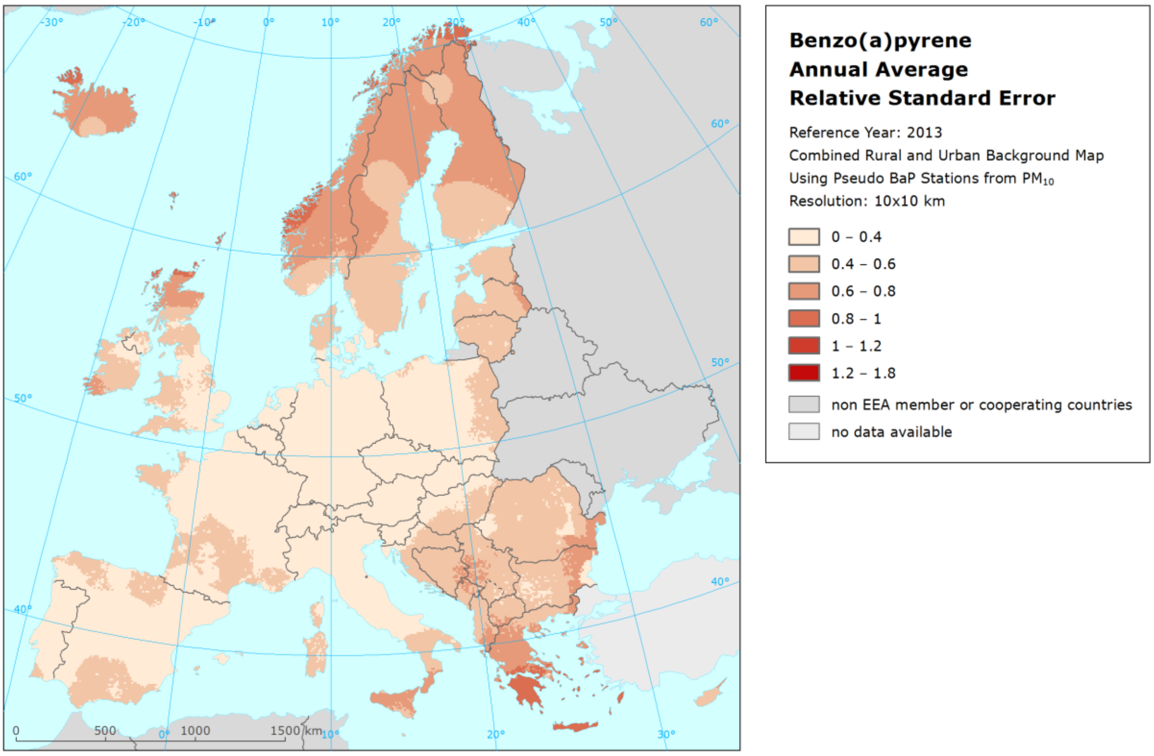

**Map 4.5** **Spatial interpolated concentration field of annual mean BaP in 2013, created using (iii) pseudo stations based on $PM_{2.5}$ (top) and uncertainty map showing relative standard error for this map (bottom). Units: $ng.m^{-3}$.**

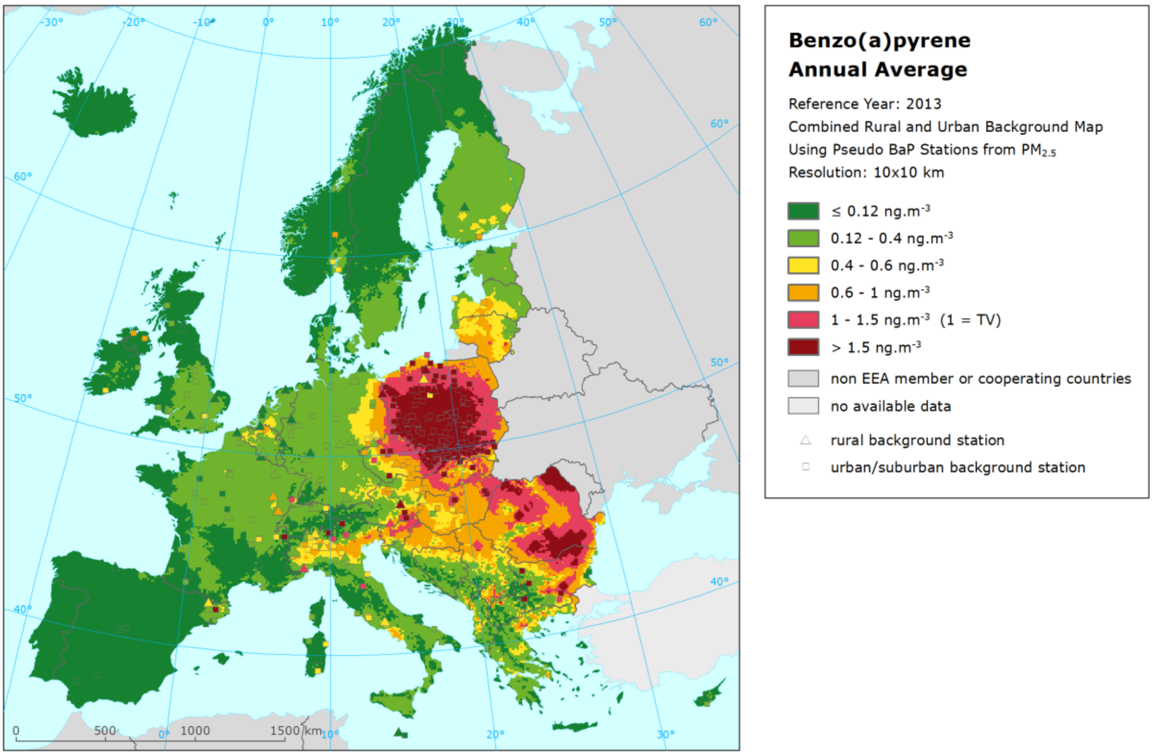


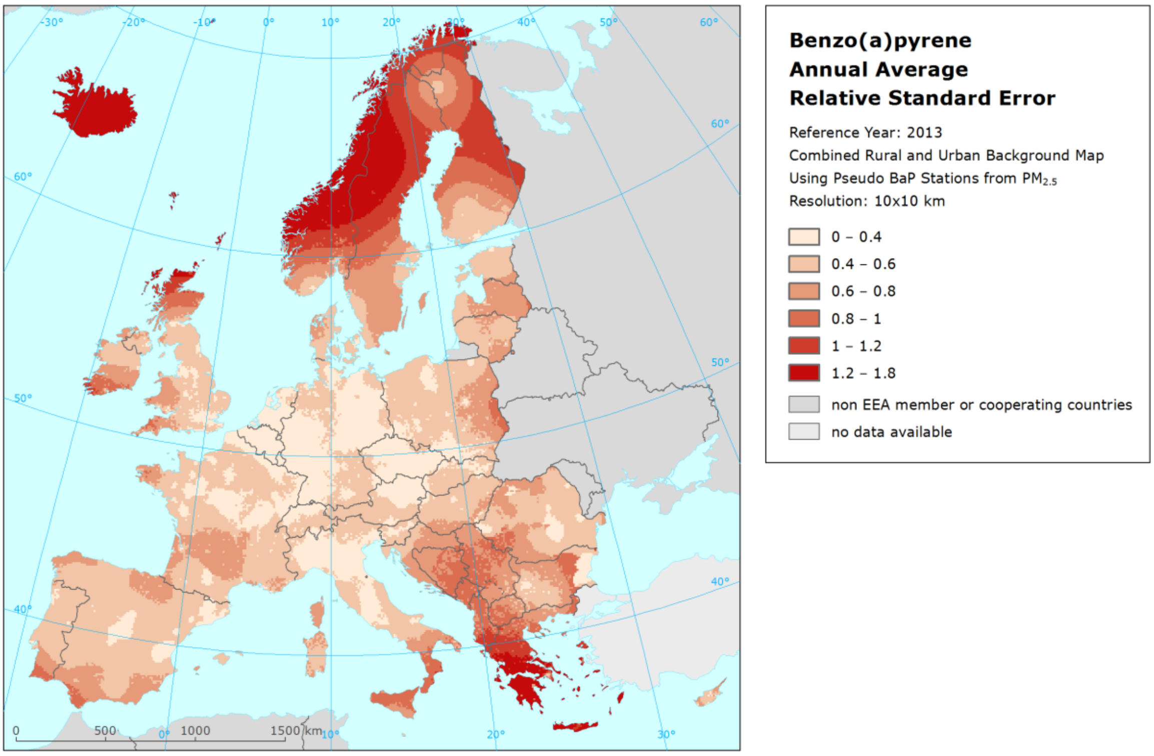

**Map 4.6 Spatial interpolated concentration field of annual mean BaP in 2013, created by (iv) method using $PM_{2.5}$ rural and urban background maps (top) and uncertainty map showing interpolation relative standard error for this map (bottom). Units: $ng.m^{-3}$.**

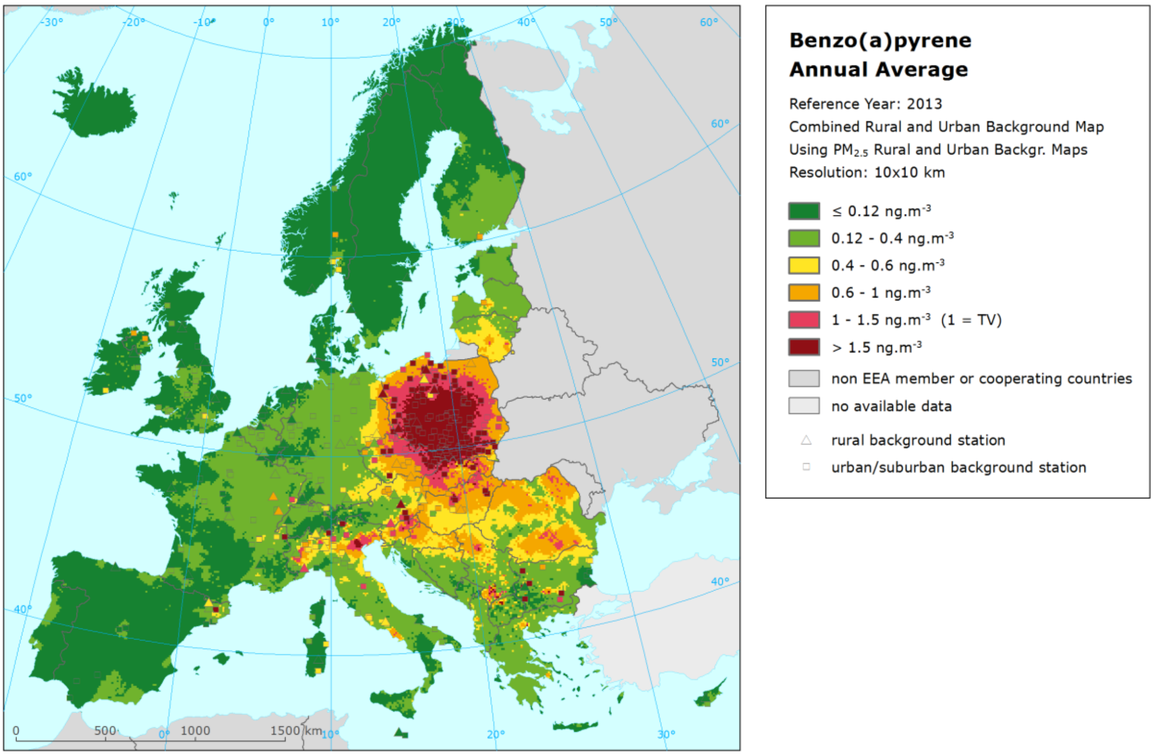


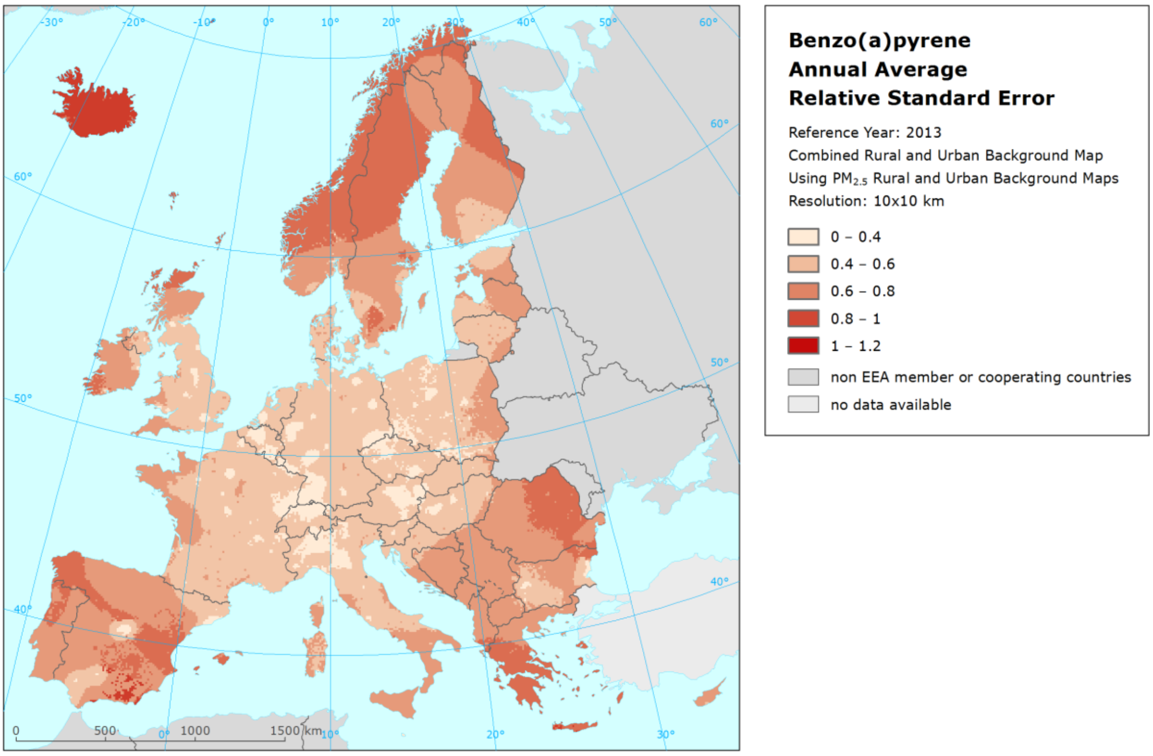

**Map 4.7** **Spatial interpolated concentration field of annual mean BaP in 2013, created by (i) current methodology (top) and (ii) using pseudo stations based on $PM_{10}$ (bottom), limited for areas with a relative uncertainty under 0.60. Units: $ng.m^{-3}$.**

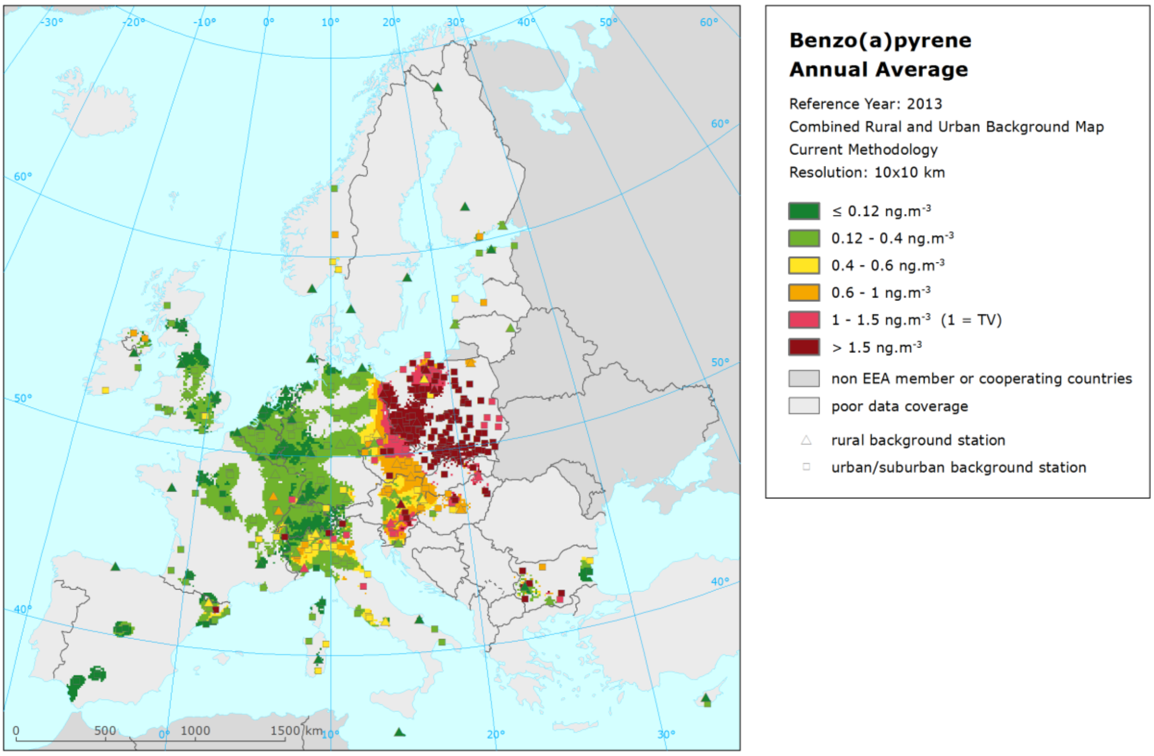


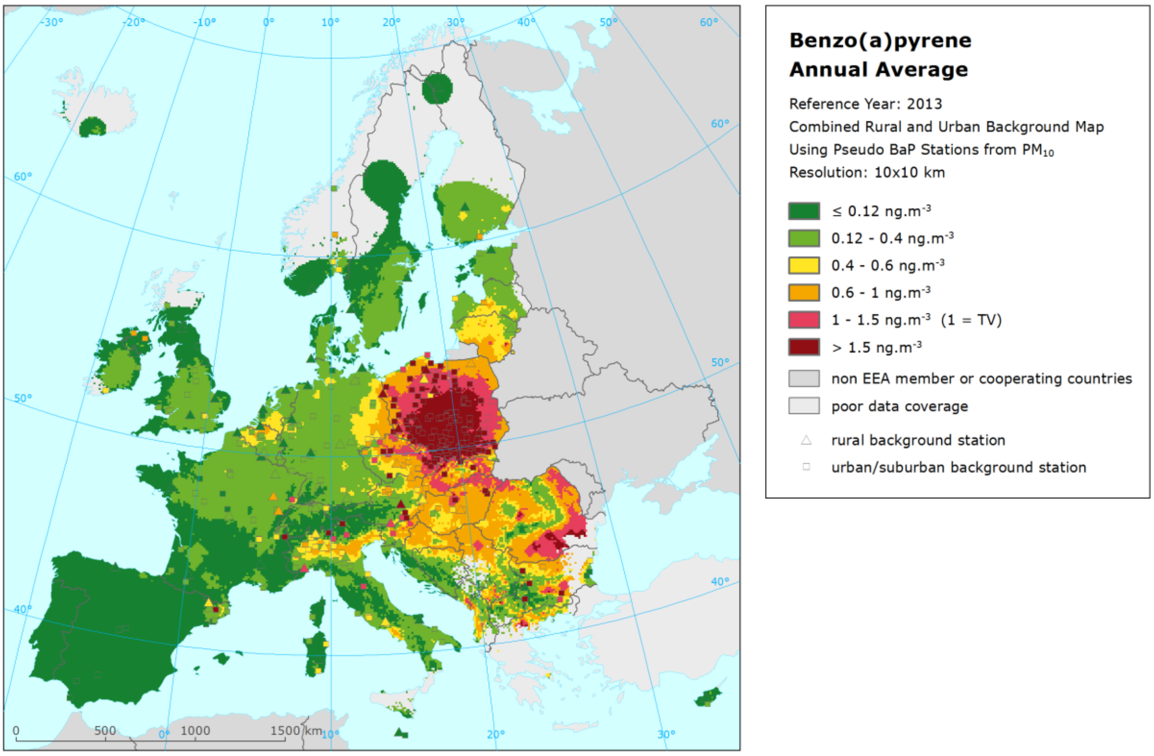

**Map 4.8** **Spatial interpolated concentration field of annual mean BaP in 2013, created by method (iii) using pseudo stations based on $PM_{2.5}$ (top) and (iv) using $PM_{2.5}$ rural and urban background maps (bottom), limited for areas with a relative uncertainty under 0.60. Units: ng.m$^{-3}$.**

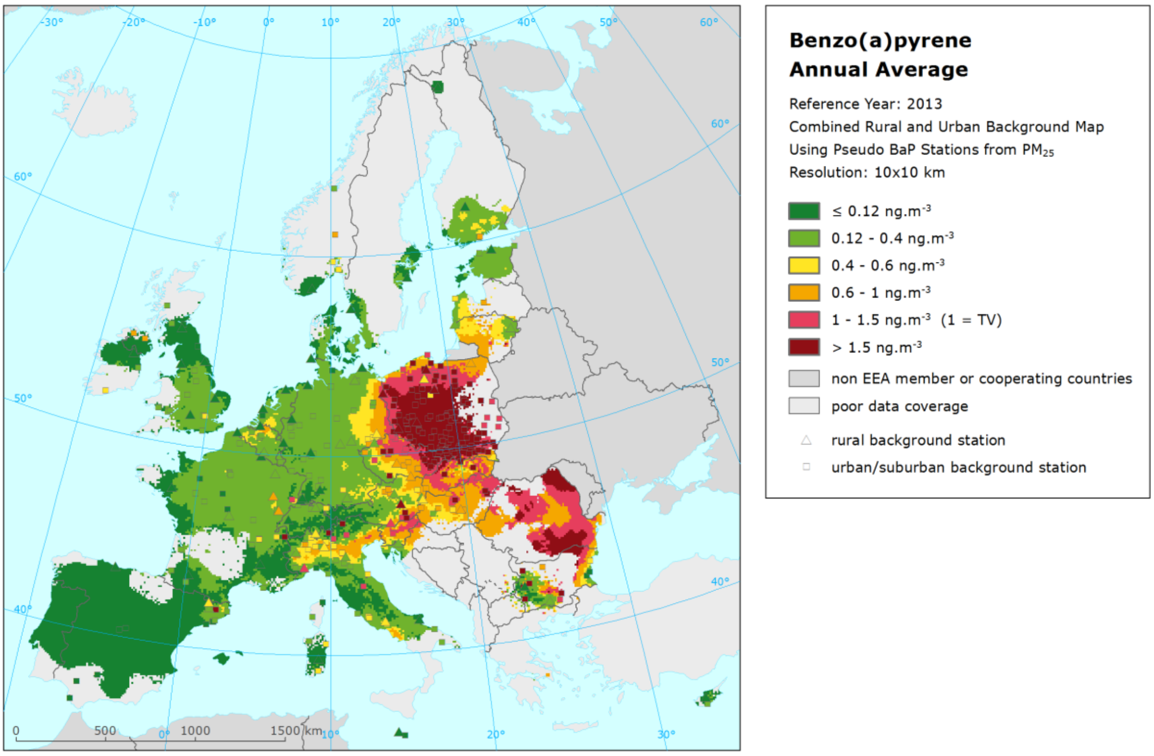


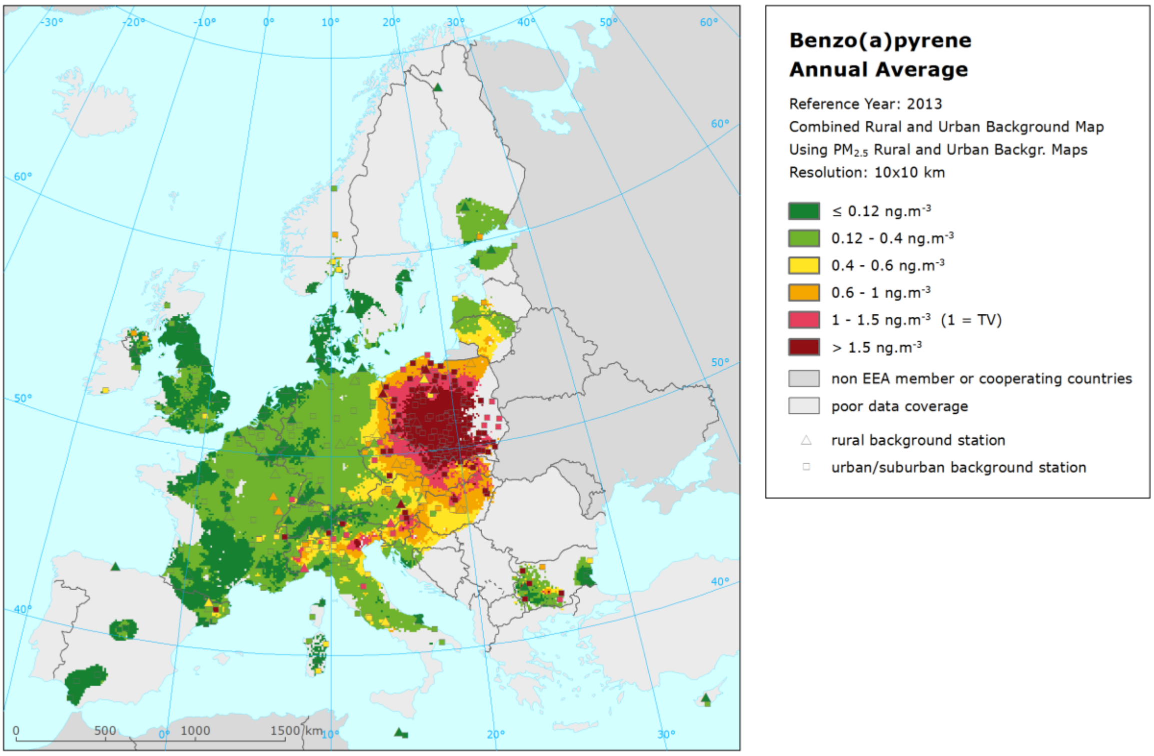

# 5 Conclusions

The paper examines the potential improvement of the BaP mapping using the pseudo BaP station data approach. Two options of the application of such pseudo-station approach for BaP mapping are examined: one based on the data from $PM_{10}$ stations and another based on $PM_{2.5}$ stations. Additionally, an alternative approach using the $PM_{2.5}$ rural and urban background maps as additional supplementary variables in the current mapping method is considered.

The analysis of the pseudo BaP station data approach shows quite high uncertainty of such estimates. The fraction of the stations with predictions within ± 50% of the observed BaP for concentrations above LAT (i.e. 0.40 $ng.m^{-3}$) and within ± 100% for concentrations below or equal to LAT is 0.63 resp. 0.74 (for the rural resp. urban areas) for the $PM_{10}$ variant and 0.61 resp. 0.69 for the $PM_{2.5}$ variant. It can be stated that this fraction of the "satisfactory" estimates is too low, compared to 0.95 required by the EC Directive for monitoring. Thus, it looks that the use of pseudo-stations has some limitations. However, regardless these limitations, we further examined the use of the pseudo BaP stations in the mapping as potential beneficial.

The BaP maps created based on four different approaches were compared using cross-validation. The map using pseudo stations based on $PM_{2.5}$ observations gives better results than the map using pseudo stations based on $PM_{10}$ observations. Both the two pseudo stations methods provide better results in the rural areas and slightly worse results in the urban areas, compared to the current mapping method. The best results are given by the method using $PM_{2.5}$ rural and urban background maps.

Next to the cross-validation, the maps created based on the four different methods were compared in the means of their relative interpolation standard error. The best results are given by the method using pseudo stations based on $PM_{10}$, the second best results are shown by the method using pseudo stations based on $PM_{2.5}$. The main reason is in the number of the stations: the use of the pseudo stations in the interpolation decreases the interpolation error. However, it should be noted that the relative standard error is probably somewhat underestimated for methods using the pseudo BaP stations, as these stations do not satisfy the requirement of the EC Directive for monitoring, as stated above.

Taking into account both the cross-validation and the relative standard error results, the most promising – for the time being with the lack of the BaP stations – seems to be the method (iii) using pseudo stations based on $PM_{2.5}$. Furthermore, this method could be potentially improved by including the pseudo $PM_{2.5}$ stations (Horálek et al., 2016), in order to increase the number of the pseudo BaP stations.

Large uncertainties are still associated with the current assessment of BaP concentrations in Europe. As indicated by Guerreiro et al. (2015), two main improvements are needed in order to reduce the uncertainties related to mapping BaP concentrations: 1) improve the quality and completeness of the BaP emission inventory; 2) improve the monitoring network over Europe for BaP concentrations, especially in areas with expected higher concentrations (e.g. in the Balkan and Baltic countries). The EMEP or other CTM modelled concentrations are very sensitive to the input emission data, and measurement data is crucial for understanding the behaviour of BaP in the atmosphere, as well as to test and validate models. Furthermore, the mapping methodology would be greatly improved by an increase in availability of BaP measurements, especially in areas of low measurement density and regions with expected concentrations above LAT.

# References


Cressie, N., 1993, *Statistics for spatial data*, Wiley series, New York.

Denby, B., Horálek, J., de Smet, P., de Leeuw, F., 2011, 'Mapping annual mean $PM_{2.5}$ concentrations in Europe: application of pseudo $PM_{2.5}$ station data', *ETC/ACM Technical Paper* 2011/5. http://acm.eionet.europa.eu/reports/ETCACM_TP_2011_5_spatialPM2.5mapping accessed 24 June 2016.

De Smet, P., Horálek, J., Coňková, M., Kurfürst, P., de Leeuw, F., Denby, B. (2011) European air quality maps of ozone and $PM_{10}$ for 2008 and their uncertainty analysis. ETC/ACC Technical Paper 2010/10. (http://acm.eionet.europa.eu/reports/ETCACC_TP_2010_10_spatAQmaps_2008) accessed 26 June 2016.

EC, 2004, 'Directive 2004/107/EC of the European Parliament and of the Council of 15 December 2004 relating to arsenic, cadmium, mercury, nickel and polycyclic aromatic hydrocarbons in ambient air', OJ L 23, 26.1.2005, pp. 3–16.

ECMWF, 2015, 'Meteorological Archival and Retrieval System (MARS)'. (https://software.ecmwf.int/wiki/display/UDOC/MARS+user+documentation) accessed 9 September 2016.

EEA, 2011, 'Guide for EEA map layout. EEA operational guidelines', August 2011, version 4. (www.eionet.europa.eu/gis/docs/GISguide_v4_EEA_Layout_for_map_production.pdf) accessed 24 June 2016.

EEA, 2015, Air Quality e-Reporting, Air quality database. Data set for 2013. (http://www.eea.europa.eu/data-and-maps/data/aqereporting) accessed 13 April 2016.

EMEP, 2015, Data of HMs and POPs for the EMEP region (http://www.msceast.org/index.php/pollution-assessment/emep-domain-menu/data-hm-pop-menu) accessed 9 September 2015.

EMEP, 2016a, Data of HMs and POPs for the EMEP region (http://www.msceast.org/index.php/pollution-assessment/emep-domain-menu/data-hm-pop-menu) accessed 20 April 2016.

EMEP, 2016b, 'Emission data for modelling heavy metals and persistent organic pollutants', *MSC-E contribution to the joint CEIP/MSC-E technical report*. (www.msceast.org/documents/emissions_report.doc) accessed 26 June 2016.

Eurostat (2014). GEOSTAT 2011 grid dataset. Population distribution dataset. (http://ec.europa.eu/eurostat/web/gisco/geodata/reference-data/population-distribution-demography) accessed 23 September 2015.

Guerreiro, C., Horálek, J., de Leeuw, F., Couvidat, F., 2015, 'Mapping ambient concentrations of benzo(a)pyrene in Europe', *ETC/ACM Technical paper* 2014/6. (http://acm.eionet.europa.eu/reports/ETCACM_TP_2014_6_BaP_HIA) accessed 24 June 2016.

Guerreiro, C., Horálek, J., de Leeuw, F., Couvidat, F., 2016, 'Benzo(a)pyrene in Europe: Ambient air concentrations, population exposure and health effects', *Environmental Pollution* 214, 657–667.

Gusev, A., Mantseva, A., Shatalov, V., Strukov, V. (2005). Regional Multicompartment Model MSCE-POP. EMEP/MSC-E Technical Report 5/2005. (http://www.msceast.org/reports/5_2005.pdf) accessed 24 June 2016.

Gusev, A., Ilyin, I., Mantseva, I., Rozovskaya, O., Shatalov, V., Travnikov, O. (2006) Progress in further development of MSCE-HM and MSCE-POP models (implementation of the model review recommendations. EMEP/MSC-E Technical Report 4/2006. (http://www.msceast.org/reports/4_2006.pdf) accessed 24 June 2016.

Horálek, J., Denby, B., de Smet, P., de Leeuw, F., Kurfürst, P., Swart, R., van Noije, T., 2007, 'Spatial mapping of air quality for European scale assessment', *ETC/ACC Technical paper* 2006/6. (http://acm.eionet.europa.eu/reports/ETCACC_TechnPaper_2006_6_Spat_AQ) accessed 9 June 2016.

Horálek, J., de Smet, P., de Leeuw, F., Conkova, M., Denby, B., Kurfürst, P., 2010, 'Methodological improvements on interpolating European air quality maps', *ETC/ACC Technical paper* 2009/16. (http://acm.eionet.europa.eu/reports/ETCACC_TP_2009_16_Improv_SpatAQmapping) accessed 9 June 2016.

Horálek, J., de Smet, P., Kurfürst, P., de Leeuw, F., Benešová, N., 2016, 'European air quality maps of PM and ozone for 2013 and their uncertainty', *ETC/ACM Technical Paper* 2015/5. (http://acm.eionet.europa.eu/reports/ETCACM_TP_2015_5_AQMaps2013) accessed 24 June 2016.

JRC, 2009, 'Population density disaggregated with Corine land cover 2000. 100x100 m grid resolution', EEA version popu01clcv5.tif of 24 Sep 2009. (http://www.eea.europa.eu/data-and-maps/data/population-density-disaggregated-with-corine-land-cover-2000-2) accessed 9 September 2016.

ORNL, 2008, 'ORNL LandScan high resolution global population data set'. (http://www.ornl.gov/sci/landscan/landscan_documentation.shtml) accessed 9 September 2016.

# Annex I Additional measurement data

In the paper, the monitoring data extracted from the Air Quality e-Reporting database 2013 dataset (EEA, 2015) was supplemented with additional data. The additional data came from two different sources: Primarily, these were BaP and PM data submitted to the Air Quality e-Reporting database after the publishing of the 2013 dataset (EEA, 2015), provided by EEA. Second, these were BaP data from several Slovak stations, provided by SHMI. Tables A1.1 and A1.2 present the additional data used in the paper.

### Table A1.1 Additional BaP annual average data for 2013

| EoI_code | Station name | latitude | longitude | elevation | station type | area type | BaP |
|---|---|---|---|---|---|---|---|
| IT0804A | CITTADELLA | 44.7936 | 10.3317 | 60 | background | urban | 0.24 |
| IT0892A | GIARDINI MARGHERITA | 44.4833 | 11.3550 | 43 | background | urban | 0.18 |
| IT1043A | MARECCHIA | 44.0625 | 12.5533 | 6 | background | urban | 0.47 |
| IT1771A | PARCO FERRARI | 44.6517 | 10.9264 | 34 | background | urban | 0.33 |
| SK0038A | Koliba | 48.1750 | 17.1167 | 450 | Background | urban | 0.98 |
| SK0028A | Krompachy - Lorenzova | 48.9122 | 20.8725 | 387 | Background | urban | 2.82 |
| SK0012A | Prievidza - J. Hollého | 48.7697 | 18.6231 | 283 | Background | urban | 1.90 |

### Table A1.2 Additional $PM_{10}$ and $PM_{2.5}$ annual average data for 2013

| EoI code | Station name | latitude | longitude | altitude | station type | area type | $PM_{10}$ | $PM_{2.5}$ |
|---|---|---|---|---|---|---|---|---|
| IT0854A | CORSO FIRENZE - GENOVA 701009 | 44.4181 | 8.9275 | 105 | Background | urban | 16.9 | |
| IT0858A | QUARTO - GENOVA 701016 | 44.3964 | 8.9922 | 85 | Background | urban | 15.0 | 9.0 |
| IT0862A | FI-BASSI 904809 | 43.7867 | 11.2875 | 61 | Background | urban | 20.1 | 14.0 |
| IT0948A | FI-BOBOLI 904810 | 43.7653 | 11.2492 | 75 | Background | urban | 20.0 | |
| IT0988A | DONNAS 200708 | 45.5975 | 7.7603 | 371 | Background | rural | 19.8 | |
| IT1071A | PI-SANTA-CROCE-COOP 905011 | 43.7131 | 10.7717 | 16 | Background | suburban | 26.7 | |
| IT1110A | PI-PASSI 905008 | 43.7389 | 10.4017 | 5 | Background | urban | 23.0 | 15.5 |
| IT1149A | PI-MONTECERBOLI 905007 | 43.2478 | 10.8817 | 353 | Background | suburban | 9.5 | |
| IT1186A | LU-VIAREGGIO 904610 | 43.8839 | 10.2450 | 3 | Background | urban | 27.0 | |
| IT1187A | LU-CAPANNORI 904601 | 43.8408 | 10.5739 | 10 | Background | urban | 24.2 | |
| IT1233A | CENGIO - CAMPO DI CALCIO 700901 | 44.3906 | 8.2014 | 400 | Background | rural | 10.5 | |
| IT1277A | CENSN1 2009106 | 40.5750 | 9.6944 | 39 | Background | urban | 15.2 | |
| IT1536A | MAGGIOLINA - LA SPEZIA 701113 | 44.1178 | 9.8428 | 6 | Background | urban | 21.5 | 13.9 |
| IT1551A | FI-SCANDICCI 904819 | 43.7569 | 11.1928 | 45 | Background | urban | 24.2 | |
| IT1553A | PT-MONTALE 904705 | 43.9161 | 11.0069 | 48 | Background | rural | 29.1 | 18.8 |
| IT1571A | PT-SIGNORELLI 904702 | 43.9408 | 10.9053 | 80 | Background | urban | 22.9 | |
| IT1593A | GR-URSS 905301 | 42.7786 | 11.1192 | 10 | Background | urban | 17.2 | 10.8 |
| IT1654A | PO-ROMA 904805 | 43.8728 | 11.0919 | 54 | Background | urban | 27.2 | 20.0 |
| IT1663A | Mesagne 1607414 | 40.5656 | 17.8083 | 10 | Background | suburban | 23.7 | |
| IT1681A | AR-CASA-STABBI 905108 | 43.6603 | 11.9017 | 650 | Background | rural | 9.4 | |
| IT1725A | AOSTA (Q.RE DORA) 200715 | 45.7339 | 7.3422 | 570 | Background | urban | 20.5 | |
| IT1819A | MS-PARCHEGGIO-COLOMBAROTTO | 44.0783 | 10.0972 | 98 | Background | urban | 23.8 | |
| IT1883A | VARALDO - SAVONA 700971 | 44.3153 | 8.4856 | 55 | Background | urban | 17.0 | 11.9 |
| IT1962A | VENAFRO2 1409499 | 41.4789 | 14.0333 | 170 | Background | urban | 33.5 | |
| IT2005A | CEOLB1 2010401 | 40.9275 | 9.4917 | 0 | Background | suburban | 20.3 | |
| IT2009A | CENS16 2009021 | 40.7244 | 8.5761 | 275 | Background | suburban | 16.9 | 7.8 |
| IT2011A | CENSE0 2009239 | 39.8425 | 9.2164 | 736 | Background | rural | 11.2 | 5.6 |
| IT2032A | SI-POGGIBONSI 905204 | 43.4728 | 11.1419 | 105 | Background | urban | 18.5 | 12.2 |
| IT2040A | CENQU1 2009240 | 39.2328 | 9.1881 | 8 | Background | urban | 31.9 | |
| IT2141A | Posta del Principe | 41.6308 | 15.3867 | 150 | background | rural | | 11.7 |

# Annex II EMEP model 2013 results with 2012 emissions

In this Annex, we present the EMEP model output for BaP annual average for 2013, but based on 2012 emissions and 2013 meteorology (EMEP, 2015), see Map A2.1. This model run is not used in the report. We present it for illustration only as it is of major importance on the timeliness of BaP map delivery: the map creation could be potentially accelerated when using the model with emissions of the last-but-most-recent year. (For discussion of using the model Y with Y-1 emissions in PM and ozone mapping, see Horálek et al., 2016, Annex 3.)

Comparing Map A2.1 with Map 3.2, one observes the differences in concentration levels for some areas, such as Spain, Portugal, northern Italy and Romania. The difference is solely caused by the differences in emissions for 2012 and 2013 and is illustrative for the high variability in emission data from one year to another. It can be seen the model is highly sensitive to the emission year accounted for.

**Map A2.1 Output of EMEP chemical transport model. BaP annual average in 2013, based on 2012 emission. Units: ng.m$^{-3}$.**